Nuclear structure in strong magnetic fields: Nuclei in the crust of a magnetar

D. Peña Arteaga,[1] M. Grasso,[1] E. Khan,[1] and P. Ring[2]
[1]*Institut de Physique Nucléaire, Université Paris-Sud, IN2P3-CNRS, F-91406 Orsay Cedex, France*
[2]*Physikdepartment, Technische Universität München, D-85748, Garching, Germany*
(Received 14 September 2010; revised manuscript received 26 July 2011; published 19 October 2011)

Covariant density functional theory is used to study the effect of strong magnetic fields, up to the limit predicted for neutron stars (for magnetars $B \approx 10^{18}$ G), on nuclear structure. All new terms in the equation of motion resulting from time-reversal symmetry breaking by the magnetic field and the induced currents, as well as axial deformation, are taken into account in a self-consistent fashion. For nuclei in the iron region of the nuclear chart it is found that fields on the order of magnitude of 10^{17} G significantly affect bulk properties such as masses and radii.

DOI: 10.1103/PhysRevC.84.045806 PACS number(s): 21.10.Dr, 21.60.Jz, 26.60.Gj

I. INTRODUCTION

Several studies (e.g., Refs. [1,2]) have determined the presence of intense magnetic fields, up to 10^{16} G, on the surface of neutron stars. Theoretical models suggest that these magnetic fields might reach up to $B \approx 10^{18}$ G and even larger values if one considers the limit imposed by the virial theorem ($B \approx 2 \times 10^{18}$ G [3]). The influence of the magnetic fields on the equation of state (EOS) has been thoroughly studied and reported in recent years (e.g., Refs. [3–6]). It should be noted that magnetic fields of the order of 10^{18} G can strongly influence the low-density regions of a neutron star.

The outer crust is fundamentally composed of well-separated nuclides, and its structure determined by the energies of isolated nuclei, the kinetic energy of electrons, and the lattice energy. Thus, its composition depends very much on the binding energy of stable and unstable nuclei. At the lowest densities it is thought that the most abundant component is ^{56}Fe because of its high binding energy, a fact actually observed in emission spectra (e.g., Ref. [7]).

The magnetic field strength required to directly influence the EOS can be estimated by considering its effects on charged particles. Charge-neutral, β-equilibrated neutron star matter contains both negatively charged leptons (electrons and muons) and protons. Magnetic fields quantize the orbital motion (Landau quantization) of these charged particles. When the Fermi energy of the proton becomes significantly affected by the magnetic field, the composition of matter in β equilibrium is modified. This is reflected in a change of the pressure of matter. It has been found in Ref. [3] that this occurs for fields of approximately 10^{18} G, and that in general leads to a stiffening of the EOS.

However, there are very few studies [8,9] of the changes that these very intense magnetic fields may eventually bring to the composition of the crust. The structure and composition of the crust is important in the thermal and rotational evolution of neutron stars, in particular in the theory behind glitches [1]. Some other studies [10,11] point to a magnetically driven crust activity as the source of soft γ repeaters (SGRs).

So far, the impact of intense magnetic fields in nuclei found in the outer crust has been studied on a qualitative way using a simple non-self-consistent method by Kondratyev and collaborators [8,9]. It was found that fields as low as 10^{16} G may modify the nuclear shell structure, well within the range of theoretically possible magnetic strengths. There are, however, still some questions that need to be addressed: (i) What is the minimum field that is able to significantly alter the nuclear structure? (ii) Is this field low enough to be found in a significant proportion of neutron stars or magnetars? (iii) Is this effect big enough to influence astrophysically relevant situations and processes, for example, neutron star outer crust composition or final element abundances in nucleosynthesis scenarios?

The objective of the present work is to try to find answers to these questions, in a quantitative way if possible, using a fully microscopic description of the nuclear system within covariant density functional theory. The formalism used is introduced in Sec. II. A general discussion of the effects of the external magnetic field on nuclei is given in Sec. III and particularized to an example nucleus. A discussion of the possible influence of the magnetic fields on neutron star outer crust nuclei can be found in Sec. IV. Finally, Sec. V is devoted to the conclusions.

II. FORMALISM

Covariant density functional theory starts from an effective Lagrangian that includes the nucleon and as many meson fields as needed to reproduce basic nuclear properties such as saturation (a detailed discussion can be found in Refs. [12,13]):

$$\mathcal{L} = \mathcal{L}_N + \mathcal{L}_m + \mathcal{L}_{\text{int}} + \mathcal{L}_{BO} + \mathcal{L}_{BM}. \tag{1}$$

$\mathcal{L}_N$ refers to the Lagrangian of the free nucleon

$$\mathcal{L}_N = \bar{\psi}(i\gamma^\mu \partial_\mu - m)\psi, \tag{2}$$

where m is the bare nucleon mass and ψ denotes the Dirac spinor. $\mathcal{L}_m$ is the Lagrangian of the free meson fields and the electromagnetic field generated by the protons

$$\begin{aligned}\mathcal{L}_m = {} & \tfrac{1}{2}\partial_\mu\sigma\partial^\mu\sigma - \tfrac{1}{2}m_\sigma^2\sigma^2 - \tfrac{1}{4}\Omega_{\mu\nu}\Omega^{\mu\nu} + \tfrac{1}{2}m_\omega^2\omega_\mu\omega^\mu \\ & - \tfrac{1}{4}\vec{R}_{\mu\nu}\vec{R}^{\mu\nu} + \tfrac{1}{2}m_\rho^2\vec{\rho}_\mu\vec{\rho}^\mu - \tfrac{1}{4}F_{\mu\nu}F^{\mu\nu} + U(\sigma),\end{aligned} \tag{3}$$

where m_σ, m_ω, and m_ρ are the meson masses, and $U(\sigma) = (g_2/3)\sigma^3 + (g_3/4)\sigma^4$ is the standard form for the nonlinear

coupling of the σ meson field. The interaction Lagrangian $\mathcal{L}_{\rm int}$ is given by minimal coupling terms

$$\mathcal{L}_{\rm int} = -g_\sigma \bar\psi \sigma \psi - g_\omega \bar\psi \gamma^\mu \omega_\mu \psi - g_\rho \bar\psi \gamma^\mu \vec\tau \vec\rho_\mu \psi - e\bar\psi \gamma^\mu A_\mu \psi, \quad (4)$$

where g_σ, g_ω, g_ρ, and e are the respective coupling constants for the σ, ω, $\vec\rho$, and photon fields and, of course, e vanishes for neutrons. In the previous and subsequent formulas, bold symbols denote vectors in ordinary space, and arrows denote vectors in isospin space. These three terms, $\mathcal{L}_N$, $\mathcal{L}_m$, and $\mathcal{L}_{\rm int}$, compose the standard RMF Lagrangian. Throughout this work the parameter set NL3 [14] is used for the masses and coupling constants of the model. This parameter set has been thoroughly used and has led to very successful description of many nuclear properties. In addition, there are two new terms corresponding to the interaction of the nuclear system with an external magnetic field: (i) the coupling of the proton orbital motion with the external magnetic field,

$$\mathcal{L}_{BO} = -e\bar\psi \gamma^\mu A^{(e)}_\mu \psi, \quad (5)$$

and (ii) the coupling of both proton and neutron intrinsic dipole magnetic moments with the external magnetic field [15]

$$\mathcal{L}_{BM} = -\bar\psi \chi^{(e)}_{\tau_3} \psi, \quad (6)$$

where

$$\chi^{(e)}_{\tau_3} = \kappa_{\tau_3} \mu_N \tfrac{1}{2} \sigma_{\mu\nu} F^{(e)\mu\nu}. \quad (7)$$

Here $\sigma_{\mu\nu} = \frac{i}{2}[\gamma_\mu, \gamma_\nu]$ and $\mu_N = e\hbar/2m$ is the nuclear magneton and $\kappa_n = g_n/2$, $\kappa_p = g_p/2 - 1$, with $g_n = -3.8263$ and $g_p = 5.5856$, are the intrinsic magnetic moments of protons and neutrons. Interactions with the external magnetic field are marked the superscript (e). This field is considered to be externally generated, and therefore there is no associated field equation and thus no other bosonic terms in the Lagrangian. Both terms $\mathcal{L}_{BO}$ (5) and $\mathcal{L}_{BM}$ (6) have to be taken into account because at the magnetic field strengths of interest ($B \approx 10^{17}$ G) they are of the same order of magnitude.

The Hamiltonian density can be derived from the Lagrangian density of Eq. (1) as the (0,0) component of the energy-momentum tensor, leading the to the energy functional $E_{\boldsymbol{B}}[\hat\rho, \phi]$ (see in Ref. [13] for details):

$$E_{\boldsymbol{B}}[\hat\rho, \phi] = \mathrm{Tr}\left\{\left[\boldsymbol{\alpha}(-i\boldsymbol{\nabla} - e\boldsymbol{A}^{(e)}) + \beta\left(m + \chi^{(e)}_{\tau_3}\right)\right]\hat\rho\right\} + \sum_m \mathrm{Tr}\left[(\beta\, \boldsymbol{\Gamma}_m \phi_m)\, \hat\rho\right] \pm \sum_m \int d^3r \left[\frac{1}{2}(\partial_\mu \phi_m)^2 + \frac{1}{2} m_m^2 \phi_m^2\right], \quad (8)$$

where the upper sign holds for scalar and the lower sign for vector mesons;

$$\hat\rho(\boldsymbol{r}) = \sum_i |\psi_i(\boldsymbol{r})\rangle\langle\psi_i(\boldsymbol{r})| \quad (9)$$

is the relativistic single-particle density matrix and the traces run over the Dirac indices and over the integral in r pace and, according to the no-sea approximation, the index i runs over all the occupied levels in the Fermi sea. The index $m = \sigma, \omega, \rho, e$ runs over the various meson and electromagnetic fields and the vertices Γ_m read

$$\Gamma_\sigma = g_\sigma, \qquad \Gamma^\mu_\omega = g_\omega \gamma^\mu, \qquad \vec\Gamma^\mu_\rho = g_\rho \vec\tau \gamma^\mu, \qquad \Gamma^\mu_e = e\gamma^\mu, \quad (10)$$

and $\frac{1}{2} m_m^2 \phi_m^2$ has to be replaced by $\frac{1}{2} m_\sigma^2 \sigma^2 + U(\sigma)$ in the case of the σ meson. It is customary at this point to introduce an additional term into the energy functional to account for pairing correlations [16], at least in its simplest BCS approximation. In the present study, however, pairing effects are completely neglected. It is a well-known fact [17] that static magnetic fields lead to a reduction in pair correlations in superconductors and to the appearance of a critical field where all such correlations vanish.

The functional (8) follows the spirit of magnetic-field-and-density functional theory (BDFT) [18], in which the vector potential is introduced as an explicit dependence in the energy functional. Considering that astrophysical magnetic fields can be taken as constant on a nuclear scale (i.e., their functional form is fixed), it would be of little advantage to use the more general current-and-density functional theory (CDFT) [19], which generalizes density functional theory (DFT) with the inclusion of an external vector potential in a universal fashion. Because there is no practical value in considering the external magnetic field $\boldsymbol{B}$ as an independent variable, it is regarded in the density functional as a parametric variable. Minimization with respect to the density $\hat\rho$ in the Hartree approximation [13] and considering only static configurations leads to the stationary Dirac equation for the nucleons and to the Klein-Gordon equations for the mesons

$$\hat h_D \psi_i = \epsilon_i \psi_i, \quad (11)$$

$$\left[-\Delta + m_m^2\right]\phi_m = \mp \sum_i \bar\psi_i \Gamma_m \psi_i, \quad (12)$$

where m_m^2 has to be replaced by $m_\sigma^2 + g_2\sigma + g_3\sigma^2$ in the case of the σ meson and where the Dirac Hamiltonian has the form

$$\hat h_D = \frac{\delta E_B[\hat\rho, \phi]}{\delta \hat\rho} = \boldsymbol{\alpha}(-i\boldsymbol{\nabla} - \mathbf{V}) + V_0 + \beta(m + S) + \beta\chi^{(e)}_{\tau_3}, \quad (13)$$

with the scalar and vector potentials S and V_μ defined as

$$S = -g_\sigma \sigma, \quad (14)$$

$$V_\mu = g_\omega \omega_\mu + g_\rho \tau_3 \rho_{\mu,3} + eA_\mu + eA^{(e)}_\mu. \quad (15)$$

At this point it may be useful to fix the functional form of the magnetic field. Of course, it is not constant throughout the neutron star. However, the scale of changes is much larger than the microscopic nuclear scale [3]. Thus, the magnetic field $\boldsymbol{B}$ within each individual nucleus might be considered constant. If one chooses the intrinsic z axis in the direction of this constant external magnetic field $\boldsymbol{B} = (0, 0, B)$ and cylindrical coordinates (z, r, φ) the contribution of this external field to the vector potential $\mathbf{V}$ can be written, in the symmetric gauge, as

$$\boldsymbol{A}^{(e)} = -\frac{rB}{2}\boldsymbol{e}_\varphi, \quad (16)$$

where $\boldsymbol{e}_\varphi$ is the unit vector associated with the azimuth angle φ and r is the distance from the symmetry axis. As discussed in Eq. (B3) of the Appendix B the contribution of the intrinsic magnetic moments is given by

$$\chi_{\tau_3}^{(e)} = -\kappa_{\tau_3}\mu_N \Sigma_3 B. \tag{17}$$

It is clear that the presence of the magnetic field breaks spherical symmetry for the Dirac and Klein-Gordon equations. Only axial symmetry is preserved for fields of the form (16). As discussed in Ref. [12] the spinor solutions in Eq. (11) can be written, in axial symmetry, as

$$|\psi_i(\boldsymbol{r})\rangle = \frac{1}{\sqrt{2\pi}} \begin{pmatrix} f_i^+(r,z)e^{i(\Omega_i-1/2)\varphi} \\ f_i^-(r,z)e^{i(\Omega_i+1/2)\varphi} \\ ig_i^+(r,z)e^{i(\Omega_i-1/2)\varphi} \\ ig_i^-(r,z)e^{i(\Omega_i+1/2)\varphi} \end{pmatrix} \chi_{t_i(t)}. \tag{18}$$

They are characterized by the angular momentum projection Ω, the parity π, and the isospin projection t. For even-even nuclei and in the absence of an external magnetic field, according to Kramers rule, for each solution ψ_i with positive Ω_i there exists a time-reversed one with the same energy, denoted by a bar, $\bar{\imath} := \{\epsilon_i, -\Omega_i, \pi_i\}$. However, time-reversal symmetry is broken by the magnetic field, so the twofold degeneracy is not present and one needs to consider both solutions separately. This breaking of time-reversal symmetry in the intrinsic frame leads to the appearance of time-odd mean fields and nonvanishing currents which induce spacelike components of the vector mesons ω and ρ, usually referred to as nuclear magnetism [20–22]. It is a great advantage in relativistic nuclear density functionals that these time-odd mean fields are determined by the same coupling constants g_ω and g_ρ as the well-determined time-even fields.

In nonrelativistic nuclear density functionals such as Skyrme [23,24] or Gogny [25] there are, in principle, also relations connecting time-even and time-odd parts through Galilean and gauge invariance [24]. However, these relations do not connect spin and spatial degrees of freedom as consistently as Lorentz invariance and, in addition, there is ambiguity, because many of these very successful functionals, still in use, are adjusted without taking them into account.

As shown in Ref. [20] for fields of the form (16) all induced currents and magnetic potentials are parallel to $\boldsymbol{e}_\varphi$ and axial symmetry is preserved as a self-consistent symmetry [26]. One can write out explicitly the Klein-Gordon equations for the time- and spacelike meson fields as

$$\begin{aligned}
\left(-\Delta + m_\sigma^2\right)\sigma &= -g_\sigma\left(\rho_s^p + \rho_s^n\right) - g_2\sigma^2 - g_3\sigma^3, \\
\left(-\Delta + m_\omega^2\right)\omega_0 &= g_\omega\left(\rho_v^p + \rho_v^n\right), \\
\left(-\Delta + m_\omega^2\right)\boldsymbol{\omega} &= g_\omega(\boldsymbol{j}^p + \boldsymbol{j}^n), \\
\left(-\Delta + m_\rho^2\right)\rho_0 &= g_\rho\left(\rho_v^p - \rho_v^n\right), \\
\left(-\Delta + m_\rho^2\right)\boldsymbol{\rho} &= g_\rho(\boldsymbol{j}^p - \boldsymbol{j}^n), \\
-\Delta A_0 &= e\rho_v^p, \\
-\Delta \boldsymbol{A} &= e\,\boldsymbol{j}^p,
\end{aligned} \tag{19}$$

where the source scalar and vector densities read

$$\begin{aligned}
\rho_s^{n,p} &= \sum_{i=1}^{N,Z} \psi_i^\dagger \beta \psi_i, \\
\rho_v^{n,p} &= \sum_{i=1}^{N,Z} \psi_i^\dagger \psi_i,
\end{aligned} \tag{20}$$

and the source currents

$$\boldsymbol{j}^{n,p} = \sum_{i=1}^{N,Z} \psi_i^\dagger \boldsymbol{\alpha} \psi_i, \tag{21}$$

where n and p refer to neutrons and protons, respectively. Equations (11) and (12) provide a closed set. Their solution has to be found iteratively, starting from a reasonable estimate of the meson fields, the Dirac equation (11) is solved yielding the single-particle spinors. From the spinors, using Eqs. (20) and (21), one obtains the densities and currents, which act as sources for the solution of the Klein-Gordon equations (19) that provide a new set of meson fields. Repeating the procedure until convergence results in the self-consistent solution of this set of equations (see Ref. [12] for details). From this solution one can calculate physical quantities such as the total energy, radii, and deformations.

The actual numerical solution of these coupled set of equations is obtained using an oscillator expansion in $N = 20$ major shells, for which further technical details can be found in Ref. [12]. Details pertaining the new terms involved in the inclusion of the coupling to an external magnetic field can be found in Appendixes A and B.

III. EFFECTS OF THE MAGNETIC FIELD ON THE NUCLEAR STRUCTURE

The effects that the coupling of protons and neutrons to an external magnetic field has on the nucleus can be classified as follows.

Neutron paramagnetism. Also known as Pauli-type magnetism, this is caused by the interaction of the magnetic field with the neutron magnetic dipole moment. It induces a relative shift of levels with neutron spins directed along the magnetic field. Because the gyromagnetic factor for neutrons is negative ($g_n = -3.8263$), configurations with the spin antiparallel to the magnetic field are energetically favored.

Proton paramagnetism. As in the case of neutrons, this comes from the interaction of the magnetic field with the proton magnetic dipole moment. However, the gyromagnetic factor for protons is positive ($g_p = 5.5856$), which favors configurations where the proton spin is parallel to the magnetic field.

Proton orbital magnetism. Also known as Landau-type magnetic response, this couples the orbital motion of protons with the magnetic field. It favors configurations where the proton angular momentum projection is oriented along the direction of the external magnetic field.

From the single-particle level point of view, there are two different effects. The orbital magnetism associated with proton ballistic dynamics removes Kramer's degeneracy in angular

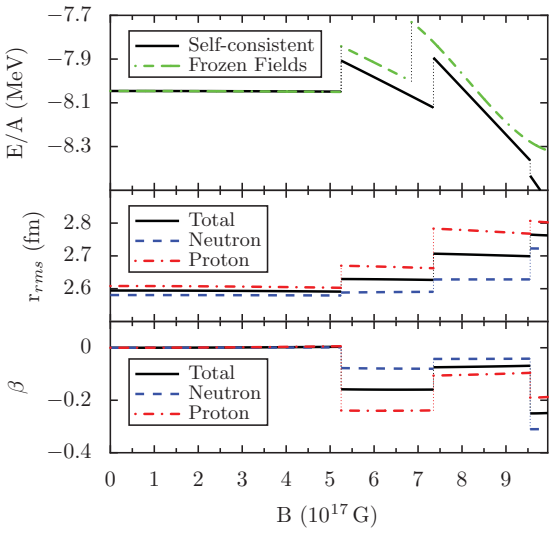

FIG. 1. (Color online) Binding energy per article, radius, and β deformation dependence on the magnetic field strength for ^{16}O. The binding energy per particle also shows the differences between using a self-consistent approach and adding the magnetic field in a frozen-field configuration on top of the bare self-consistent ground state (see text for details).

momentum projection Ω of proton levels and brings those aligned with the magnetic field down in energy. However, the paramagnetic response (Pauli magnetism) removes the angular momentum projection degeneracy for both protons and neutrons. It is thus expected that the magnetic field effect on the single-particle structure is more pronounced for protons than for neutrons.

As a first step, it is enlightening to study the effects of magnetic fields on the nuclear structure in a simple and well-known nucleus such as ^{16}O. Figure 1 shows the evolution of the bulk properties of ^{16}O with increasing magnetic field. At first the influence of the external magnetic field is counteracted by the currents generated by the breaking of time-reversal symmetry, including the classical $\propto B^2$ contribution coming from the orbital coupling. The radius of the nucleus and spherical shape show high resilience to the increase in the external magnetic field. For field strengths around 5×10^{17} G, there is an abrupt decrease in binding energy, associated with increased radius and the sudden appearance of oblate deformation for the ground state. Such discontinuities are an indication that the underlying shell structure has changed in a fundamental way. These jumps in bulk nuclear properties can be traced to the single-particle behavior, as can be observed in Figs. 2 and 3 ; they occur when the last occupied level crosses the first empty level. At that point, for even-even nuclei, a reoccupation occurs. A particle is removed from a level going upward with increasing B field and brought to a level going downward with increasing spin. Because these two levels have opposite angular momentum along the symmetry axis, the nucleus becomes spin-polarized. Another effect on the structure of nuclei which are superfluid for vanishing external magnetic field is the gradual disappearance of the neutron and proton pairing gaps with increasing external field. The original shell structure is washed out owing to the complicated pattern

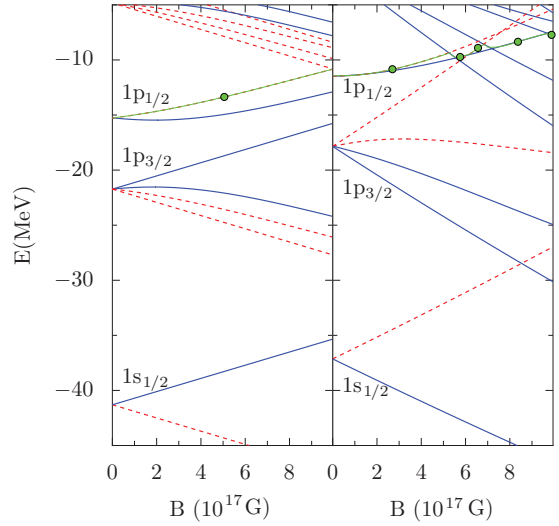

FIG. 2. (Color online) Left, neutrons; right, protons. Evolution of the single-particle levels in ^{16}O with increasing external magnetic field, with frozen nuclear potentials at their values for vanishing B. Landau coupling for the protons and the coupling of the anomalous magnetic moments is included. Blue lines refer to levels with positive angular momentum projection Ω, while red lines refer to levels with negative Ω. Solid lines indicate positive parity, while dashed lines indicate negative parity. The green dots mark the last occupied level.

of level crossings, and, as the magnetic field increases, new magic numbers may appear.

In the top panel of Fig. 1 we show two types of calculations. The full curve corresponds to self-consistent calculations, where the nuclear potentials change with increasing external fields owing to polarization of the densities and owing to the polarization currents (nuclear magnetism). The dashed curve (frozen potentials) correspond to a calculation where, in a first step, the nuclear potentials $S(\mathbf{r})$ and $V_0(\mathbf{r}) = g_\omega \omega_0(\mathbf{r}) +$

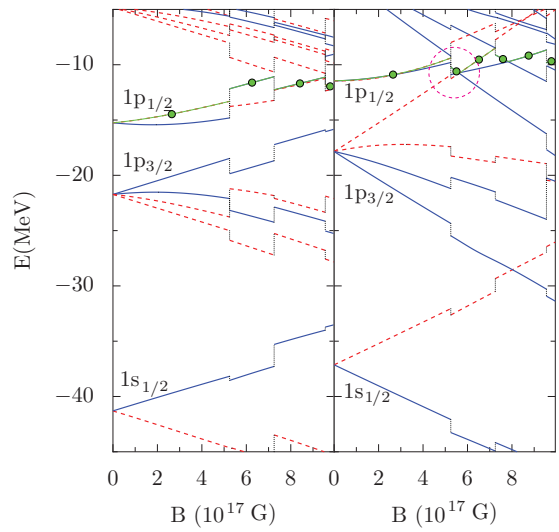

FIG. 3. (Color online) Same as Fig. 2, but with a fully self-consistent solution of the equations of motion (see text for details). The magenta circle on the proton graph highlights the first level crossing at the Fermi energy.

$g_\rho \tau_3 \rho_{0,3}(\mathbf{r}) + eA_0(\mathbf{r})$ are calculated without external magnetic field and subsequently these potentials are kept frozen while the external magnetic field is switched on. Therefore, in this case we have no nuclear magnetism. For small external fields; that is, up to the first level crossing at $B \approx 5.2 \times 10^{17}$ G there is practically no difference. Levels with $\pm\Omega$ are equally occupied and the corresponding single particle wave functions are very similar; their contributions to the currents nearly cancel each other and there is practically no polarization and no nuclear magnetism. The situation changes, however, after the first level crossing. Now the nucleus is spin polarized in the self-consistent solutions (full curve), we have polarization currents and nuclear magnetism, effects neglected in the calculations with frozen fields. Thus, we observe differences in the binding energies and also in the location of the next level crossings.

To understand the results of Fig. 1 in more detail we consider in Figs. 2 and 3 the effects on the single-particle structure outlined at the beginning of this section for frozen fields and for self-consistent fields. Proton and neutron level degeneracy is broken in reversed directions owing to the different sign in their paramagnetic behavior interacting with the external magnetic field. This degeneracy breaking is more acute in the case of protons, where the orbital magnetism plays an important role. Therefore the first level crossing occurs for the protons at $B \approx 5 \times 10^{17}$ G. For frozen fields (Fig. 2) this first level crossing for protons has no influence on the other proton levels nor on the neutron levels. This is no longer the case for the self-consistent solution in Fig. 3, where the changes in the nuclear fields caused by polarization are clearly seen also in the other proton levels and, owing to the proton-neutron interaction, also in the neutron levels.

Polarization effects induced by the ω and ρ currents owing to breaking of time-reversal symmetry are important, and the frozen fields approximation breaks down for higher magnetic fields. In the first level crossing one proton is removed from the $1p_{1/2}$ shell and brought to the downward sloping orbit of the $1d_{5/2}$ shell, that is, to a level with $\Omega = +5/2$. In the second and third panels of Fig. 1 we see that the reoccupation corresponds to an increase of the proton radius and transition from a spherical shape to an oblate deformation.

Light stable nuclei, such as ^{16}O in Fig. 1, are very stiff in their response to the external magnetic field. In this particular case the change in binding energy is less than 100 keV per particle for field strengths less than 5×10^{17} G. The induced currents tend to counteract the effects of the magnetic field. The point at which the first level crossing occurs may be arbitrarily defined as the minimum field strength for which the nuclear structure is significantly altered. Thus, for ^{16}O that would be 5×10^{17} G, with a jump in binding energy per particle of around 400 keV. For less stable and/or heavier nuclei, as is studied in the next section, it is expected that this minimum field is reduced, owing to, mainly, two effects: (i) increase in the level density around the Fermi energy, and (ii) the increase in the proton orbital magnetic response owing to the occupation of single-particle orbitals with higher angular momenta. In particular, this implies that the validity of a frozen-field treatment of the coupling to an external magnetic is highly dependent on the nucleus under consideration. In the next section the response of heavier nuclei to the external magnetic field is investigated.

IV. POSSIBLE INFLUENCE ON THE OUTER CRUST COMPOSITION

The outer crust of neutron stars, below the neutron drip density, is believed to be composed by well-separated nuclei positioned on a body-centered cubic (bcc) lattice in complete thermodynamical equilibrium. Assuming that matter in such conditions condenses to a perfect crystal lattice with a single nuclear species at each site, the energy density is [27,28]

$$\epsilon = n_N W_N(A, Z) + \epsilon'_e(n_e) + \epsilon_L(Z, n_e), \tag{22}$$

where W_N is the mass energy of the nuclear species, ϵ'_e is the free energy of the electrons, ϵ_L is the bcc Coulomb lattice energy, and n_N and n_e are the number densities of nuclei and electrons. At a given pressure, minimization of the Gibbs free energy per nucleon with respect to the nuclear species (A, Z) determines the nuclear composition of the lattice vertices.

So far all previous studies (see, for example, Refs. [3, 27–31]) on the influence of strong magnetic fields in the composition of the crust have concentrated on the electron part and assumed that the nuclear binding energy W_N is not affected. This is certainly true for weak magnetic fields below 10^{15} G, because such fields do not alter the nuclear structure. However, previous studies [8,9], where the influence of the magnetic field on the shell correction energy has been investigated in a simple model, found that fields with a strength above that threshold might change the nuclear binding energy and thus modify the equilibrium nuclear species on the lattice. In fact, changes of a few keV per nucleon might significantly alter the composition, making more neutron-rich nuclei dominate over the most likely to be found nuclei around the ^{56}Fe region [32].

One important question is the location of this magnetic field strength threshold, in particular for nuclei in the vicinity of ^{56}Fe. Assuming an electron fraction close to $Y_e = 0.5$ [33], it can be argued that the most probable nuclei are those with the same number of protons and neutrons. Figure 4 shows the dependence of the nuclear binding energy per nucleon on the magnetic field strength for $N = Z$ nuclei for fully self-consistent solutions of the RME equations in Eqs. (11) and (12)

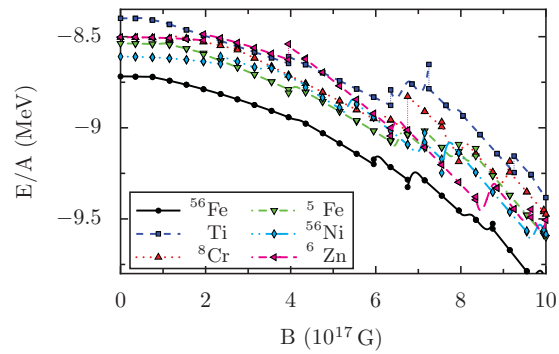

FIG. 4. (Color online) Energy per particle for $N = Z$ nuclei around ^{56}Fe.

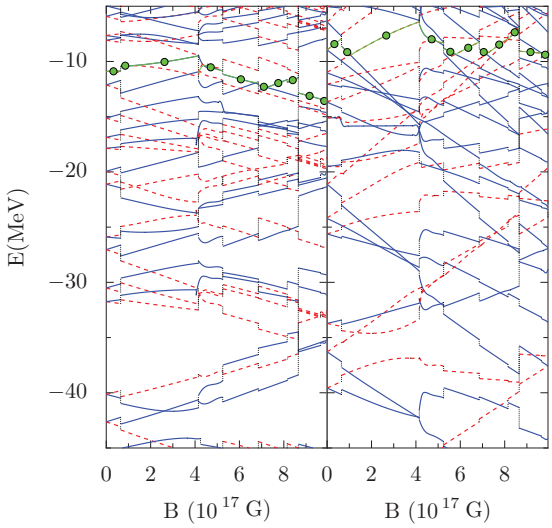

FIG. 5. (Color online) Left, neutrons; right, protons. Evolution of the single-particle levels in ^{56}Fe with the magnetic field, including the proton orbital coupling and the anomalous magnetic moments coupling. Solid (blue) lines refer to levels with positive Ω, while dashed (red) lines refer to levels with negative Ω. Solid lines indicate positive parity, while dashed lines indicate negative parity. The (green) dots mark the last occupied level.

in the region close to ^{56}Fe. For field strengths of 0.5×10^{17} G there are changes of a few tenths of a keV in the binding energy per nucleon of some species. At higher magnetic fields, around 2×10^{17} G, the hierarchy in binding energy of the most bound nuclei is altered and thus it is expected that the composition of the outer crust is substantially altered.

As in the example with ^{16}O, the origin of these discontinuities in the binding energy per particle can be traced back to the single-particle structure. Figure 5 shows the single-particle level spectra with respect to the external field for ^{56}Fe. The diagram is very similar to that of ^{16}O, only the larger level density around the Fermi energy and smaller single particle gap reduce the minimum field for which the magnetic field produces structural changes. Similar diagrams are found for all of the other nuclei presented in Fig. 5 and in those in the vicinity of ^{56}Fe. Of course, details pertaining the minimum field that induces a different single-particle level occupation scheme depend very much on each particular nucleus.

Concerning the possible changes in the hierarchy of binding energy per particle with increasing magnetic field, it has been found in this work that several nuclei (e.g., ^{57}Fe and ^{55}Fe) overbind ^{56}Fe for extended ranges of external magnetic field strengths. In that regard, the frozen field solutions show a different behavior than the self-consistent ones. The field ranges for which this hierarchy changes occur are different and the magnitude is typically off by a couple hundred keV as compared with the fully self-consistent solutions. This ordering according to binding energy is one of the factors that influences the final composition of the outer crust in neutron stars, and quantitative predictions should be done using the full self-consistent formulation.

It is also interesting to study the minimum field (defined as the field at which the first level crossing occurs) for isotopic

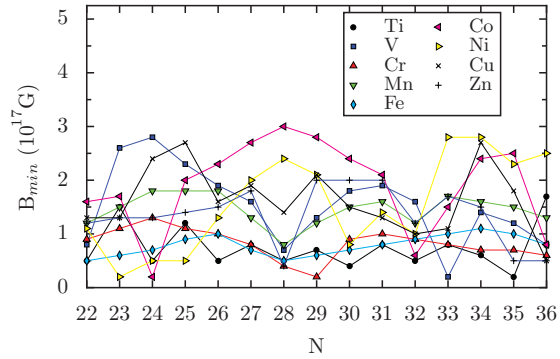

FIG. 6. (Color online) Minimum magnetic field for which the first level crossing at the Fermi energy occurs for isotopic chains around ^{56}Fe.

chains in the iron region because it provides an indication of the possible effects on the neutron star composition. Figure 6 shows the magnetic field at which the first level crossing occurs for different isotopic chains close to iron. It provides an intuitive idea of how intense the magnetic fields have to be, on average, to affect the nuclear structure significantly. For isotopes close to ^{56}Fe this value is approximately between 0.5×10^{17} and 3×10^{17} G. For heavier as well as neutron-rich nuclei, which exist at higher densities in the crust, a sharp decrease of this minimum field is expected, as mentioned previously. Thus, for fields around 10^{17} G it is reasonable to expect changes in the crust composition. However, because of the strong dependence of this minimum field on the nuclear species, it is not possible to predict the effect on the composition without actually performing the minimization of Eq. (22). This calculation is, however, computationally very demanding and would also require refinements in the model such as the inclusion of pairing (even though it is reasonable to expect that magnetic fields damp and eventually cancel it) or the proper inclusion of one-pion exchange terms in the effective Lagrangian. Therefore, it is well outside of the scope of the present work.

V. CONCLUSIONS

The influence of strong magnetic fields on nuclear structure has been studied using a fully self-consistent covariant density functional. It has been found that a field strength of at least 10^{17} G is needed to appreciably modify the nuclear ground state. For sufficiently high fields these effects cannot be studied using a frozen-field approach because there are level rearrangements, causing spin-polarization and induced currents, and thus a self-consistent model is required. It is the advantage of covariant theories that the these currents can be taken into account without any additional parameters. The minimum magnetic field that changes the nature of the nuclear ground state is very much dependent on the nucleus, and its effects on the nuclear binding energy per nucleon range from a few tenths of a keV for $B \approx 0.5 \times 10^{17}$ G to a few hundreds of keV for the maximum field theoretically possible $B \approx 10^{18}$ G.

No neutron star has yet been observed with such intense magnetic fields $B > 10^{16}$ G, even though theoretical models

hint that such objects exist [10,11]. In such a case, the composition of its outer crust might be radically different from that of normal neutron stars. The relevance of this change in composition depends on the abundance of normal neutron stars compared with that of magnetars. Until now, observations suggest that magnetars are not so common in the universe and thus it is unlikely that the magnetic field effects on nuclear structure play an important role in global astrophysical observables such as element abundances. However, changes in the composition of magnetars might be relevant in the study of different phenomena in these particular kinds of neutron stars, for example, elastic properties of the crust [34], pulsar glitches [35], or cooling [36]. With the inclusion of a proper pairing interaction, the covariant DFT model presented in this work can be used to perform a quantitative exploration of all these questions. A systematic study of changes in the composition of the outer crust will be presented in a upcoming presentation.

ACKNOWLEDGMENTS

D.P.A. is grateful to M. Urban, M. Bender, and S. Goriely for very fruitful discussions and the hospitality of the IAA group in Brussels, where part of this work was done. E.K. is grateful to N. Chamel for introducing him in the topic of this work. This paper has been supported in part by the ANR NEXEN and the DFG cluster of excellence "Origin and Structure of the Universe" (www.universe-cluster.de).

APPENDIX A: OSCILLATOR MATRIX ELEMENTS FOR THE PROTON ORBITAL COUPLING

1. Dirac equation

The Dirac equation (11) together with the meson field equations (12) are easily solved in a harmonic oscillator basis. The procedure is described in great detail in Ref. [12]. The only new term coming in the solution of the Dirac equation is $\boldsymbol{\alpha}\cdot\boldsymbol{V}$, where $\boldsymbol{V}$ is given in Eq. (15). Using the set of α matrices in the spherical tensor basis, $(\alpha_+,\alpha_-,\alpha_3)$ with

$$\alpha_+ = \begin{pmatrix} 0 & \sigma_+ \\ \sigma_+ & 0 \end{pmatrix}, \quad \alpha_- = \begin{pmatrix} 0 & \sigma_- \\ \sigma_- & 0 \end{pmatrix}, \tag{A1}$$

makes it possible to write

$$\boldsymbol{\alpha}\cdot\boldsymbol{V} = \alpha_+ V^- + \alpha_- V^+ + \alpha_3 V^3, \tag{A2}$$

with

$$\boldsymbol{A}^{(e)} = i\left(-\frac{rB}{2}e^{-i\varphi}, \frac{rB}{2}e^{i\varphi}, 0\right), \tag{A3}$$

and the internal self-consistent magnetic potential $\boldsymbol{V}$ given by the solution of the Klein-Gordon equations. Using an oscillator expansion for the spinors,

$$\psi_i = \begin{pmatrix} \sum_n f_n^i |n\rangle \\ i\sum_{n'} g_{n'}^i |n'\rangle \end{pmatrix}, \tag{A4}$$

where $|n\rangle$ are the axially symmetric harmonic oscillator wave functions, determined by the quantum numbers $n \equiv (n_z, n_r, m_l, m_s)$:

$$|n\rangle \equiv |n_z n_r m_l m_s\rangle = \phi_{n_z}(z)\phi_{n_r}^{|m_l|}(r)\frac{e^{im_l\varphi}}{\sqrt{2\pi}}\chi_{m_s}(s), \tag{A5}$$

with $\Omega = m_l + m_s$. The term $\boldsymbol{\alpha}\cdot\boldsymbol{V}$ in the Dirac equation is then in matrix form

$$\begin{pmatrix} 0 & \mathcal{B}_{nn'} \\ \mathcal{B}_{n'n} & 0 \end{pmatrix}\begin{pmatrix} f_n \\ ig_{n'} \end{pmatrix}, \tag{A6}$$

with

$$\mathcal{B}_{nn'} = -\langle n|V^-\sigma_+|n'\rangle - \langle n|V^+\sigma_-|n'\rangle. \tag{A7}$$

The oscillator matrix elements can be written as

$$\langle n|V^-\sigma_+|n'\rangle = +\delta_{m_l',m_l+1}\langle n_z n_r m_l|V^-|n_z' n_r' m_l'\rangle, \tag{A8}$$

$$\langle n|V^+\sigma_-|n'\rangle = -\delta_{m_l',m_l-1}\langle n_z n_r m_l|V^+|n_z' n_r' m_l'\rangle. \tag{A9}$$

2. Currents in coordinate space

To solve the Klein-Gordon equations, the source terms have to be transformed from oscillator to coordinate space. Expressions for the scalar and vector densities are given in Ref. [12]. The currents are defined as

$$\boldsymbol{j}(\boldsymbol{r}) = \sum_i \psi_i^\dagger(\boldsymbol{r})\boldsymbol{\alpha}\psi_i(\boldsymbol{r}). \tag{A10}$$

Because of axial symmetry the third component vanishes, and we have to consider only two of the components:

$$j_+(\boldsymbol{r}) = \sum_i \psi_i^\dagger\alpha_+\psi_i, \quad j_-(\boldsymbol{r}) = \sum_i \psi_i^\dagger\alpha_-\psi_i. \tag{A11}$$

Because $\alpha_+ = (\alpha_-)^\dagger$ we have $j_- = j_+^*$, so only one of them needs to be calculated explicitly. With the Dirac spinors in Eq. (18) we find

$$j_+(\boldsymbol{r}) = +ie^{-i\varphi}j(r,z), \tag{A12}$$

$$j_-(\boldsymbol{r}) = -ie^{+i\varphi}j(r,z), \tag{A13}$$

with

$$j(r,z) = \sum_i\sum_{nn'} f_n^i g_{n'}^i \Phi_n(r,z)\Phi_{n'}(r,z)\delta_{m_l',m_l+1} - \sum_i\sum_{nn'} f_n^i g_{n'}^i \Phi_n(r,z)\Phi_{n'}(r,z)\delta_{m_l',m_l-1}, \tag{A14}$$

where the $\Phi_n(r,z)$ are the oscillator wave functions without spin dependence; that is, $\Phi_n(r,z) = \phi_{n_z}(z)\phi_{n_r}^{|m_l|}(r)$.

3. Klein-Gordon equation oscillator matrix elements for the vector terms

In the spherical tensor basis, the Klein-Gordon (K-G) equations read

$$(-\Delta + m^2)w^i = gj^i, \qquad i = +,-,3, \tag{A15}$$

for the massive mesons. The functional form of the currents, $j_\pm(r,\theta,z) = \pm i\, j(r,z)e^{\mp i\theta}$, suggest the following ansatz for the potentials: $w_\pm(r,\theta,z) = \pm i\, w(r,z)e^{\mp i\theta}$. Inserting

both in the K-G equations and eliminating the angular dependence in θ,

$$\left(-\partial_r^2 - \frac{1}{r}\partial_r - \partial_z^2 + \frac{1}{r^2} + m^2\right) w(r,z) = j(r,z). \quad \text{(A16)}$$

The oscillator matrix elements for the Laplacian can be found in Ref. [12]. It is only a matter of including the oscillator matrix elements for the $1/r^2$ term, which can be accomplished trivially in coordinate space.

APPENDIX B: OSCILLATOR MATRIX ELEMENTS FOR THE COUPLING WITH INTRINSIC MAGNETIC MOMENTS

The coupling of the magnetic field with the anomalous magnetic moments of protons and neutrons introduces a new term in the single-particle Dirac equation (11) with

$$\chi^{(e)}_{\tau_3} = \kappa_{\tau_3}\mu_N \tfrac{1}{2}\sigma_{\mu\nu}F^{(e)\mu\nu}. \quad \text{(B1)}$$

For a constant magnetic field $\boldsymbol{B}$ of the form (16) it is easy to show that

$$\frac{1}{2}\sigma_{\mu\nu}F^{(e)\mu\nu} = -\begin{pmatrix}\boldsymbol{\sigma} & 0\\ 0 & \boldsymbol{\sigma}\end{pmatrix}\cdot\boldsymbol{B} = -\boldsymbol{\Sigma}\cdot\boldsymbol{B}, \quad \text{(B2)}$$

and for $\boldsymbol{B} = (0.0, B)$ we have

$$\chi^{(e)}_{\tau_3} = -\kappa_{\tau_3}\mu_N\Sigma_3 B, \quad \text{(B3)}$$

Finally, the oscillator matrix elements can be written as

$$\langle n|i\,\chi^{(e)}_{\tau_3}|n'\rangle = \pm\delta_{n_z n'_z}\delta_{n_r n'_r}\delta_{m_l m'_l}\delta_{m_s m'_s}\kappa_{\tau_3}\mu_N B \quad \text{(B4)}$$

for $m_s = \pm\frac{1}{2}$.

[1] S. L. Shapiro and S. A. Teukolski, *Black Holes, White Dwarfs, and Neutron Stars* (Wiley, New York, 1983).
[2] P. Haensel, A. Potekhin, and D. Yakovlev, *Neutron Stars 1: Equation of State and Structure* (Springer, Berlin, 2006).
[3] A. Broderik, M. Prakash, and J. M. Lattimer, Astrophys. J. **537**, 351 (2000).
[4] M. Guang-Jun, V. N. Kondratyev, A. Iwamoto, L. Zhu-Xia, W. Xi-Zhen, W. Greiner, and I. N. Mikhailov, Chin. Phys. Lett. **20**, 1238 (2003).
[5] F. X. Wei, G. J. Mao, C. M. Ko, L. S. Kisslinger, H. Stöcker, and W. Greiner, J. Phys. G **32**, 47 (2006).
[6] A. Rabhi, C. Providência, and J. Da Providência, J. Phys. G **35**, 125201 (2008).
[7] E. M. Cackett, J. M. Miller, S. Bhattacharyya, J. E. Grindlay, J. Homan, M. van Der Klis, M. Coleman Miller, T. E. Strohmayer, and R. Wijnands, Astrophys. J. **674**, 415 (2008).
[8] V. N. Kondratyev, T. Maruyama, and S. Chiba, Phys. Rev. Lett. **84**, 1086 (2000).
[9] V. N. Kondratyev, T. Maruyama, and S. Chiba, Astrophys. J. **546**, 1137 (2001).
[10] R. C. Duncan and H. Li, Astrophys. J. **484**, 720 (1997).
[11] C. Thompson and R. C. Duncan, Astrophys. J. **561**, 980 (2001).
[12] Y. K. Gambhir, P. Ring, and A. Thimet, Ann. Phys. (NY) **198**, 132 (1990).
[13] D. Vretenar, A. V. Afanasjev, G. A. Lalazissis, and P. Ring, Phys. Rep. **409**, 101 (2005).
[14] G. A. Lalazissis, J. König, and P. Ring, Phys. Rev. C **55**, 540 (1997).
[15] J. D. Bjorken and S. D. Drell, *Relativistic Quantum Mechanics* (McGraw-Hill, New York, 1964, 1998).
[16] H. Kucharek and P. Ring, Z. Phys. A **339**, 23 (1991).
[17] C. Kittel, *Quantum Theory of Solids* (Wiley, New York, 1963).
[18] C. J. Grayce and R. A. Harris, Phys. Rev. A **50**, 3089 (1994).
[19] G. Vignale, M. Rasold, and D. J. Geldart, Adv. Quantum Chem. **21**, 235 (1990).
[20] U. Hofmann and P. Ring, Phys. Lett. B **214**, 307 (1988).
[21] W. Koepf and P. Ring, Nucl. Phys. A **511**, 279 (1990).
[22] A. V. Afanasjev and H. Abusara, Phys. Rev. C **81**, 014309 (2010).
[23] Y. M. Engel, D. M. Brink, K. Goeke, S. J. Krieger, and D. Vautherin, Nucl. Phys. A **249**, 215 (1975).
[24] J. Dobaczewski and J. Dudek, Phys. Rev. C **52**, 1827 (1995).
[25] J. L. Egido and L. M. Robledo, Phys. Rev. Lett. **70**, 2876 (1993).
[26] P. Ring and P. Schuck, *The Nuclear Many-Body Problem* (Springer-Verlag, Berlin, 1980).
[27] P. Haensel, J. L. Zdunik, and J. Dobaczewski, Astron. Astrophys. **222**, 353 (1989).
[28] D. Lai and S. L. Shapiro, Astrophys. J. **383**, 745 (1991).
[29] U. Geppert, M. Küker, and D. Page, Astron. Astrophys. **427**, 267 (2004).
[30] U. Geppert, M. Küker, and D. Page, Astron. Astrophys. **457**, 937 (2006).
[31] G. Jie, L. Zhi-Quan, L. Wei-Wei, and L. Gang, Chin. Phys. B **19**, 099701 (2010).
[32] S. Goriely (private communication).
[33] S. E. Woosley, A. Heger, and T. A. Weaver, Rev. Mod. Phys. **74**, 1015 (2002).
[34] C. J. Pethick and A. Y. Potekhin, Phys. Lett. B **427**, 7 (1998).
[35] Y. Mochizuki and T. Izuyama, Astrophys. J. **440**, 263 (1995).
[36] F. V. DeBlasio and G. Lazzari, Phys. Rev. C **52**, 418 (1995).